

# Macroscopic evidence of energy gap in single walled carbon nanotube bundles

M. Salvato<sup>a,b</sup>, M. Cirillo<sup>a</sup>, M. Lucci<sup>a</sup>, S. Orlanducci<sup>c</sup>, I. Ottaviani<sup>a</sup>, M.L. Terranova<sup>c</sup>, and F. Toschi<sup>c</sup>

<sup>a)</sup> *Dipartimento di Fisica and MINAS Laboratory, Università di Roma “Tor Vergata”, I- 00133 Roma*

<sup>b)</sup> *Laboratorio Regionale “Super Mat” CNR-INFN, I-84081, Baronissi, Italy*

<sup>c)</sup> *Dipartimento di Scienze e Tecnologie Chimiche and MINAS Laboratory, Università di Roma “Tor Vergata”, I- 00133 Roma*

## Abstract

We report on experiments conducted on single walled nanotube bundles aligned in chains and connected through a natural contact barrier. The current-voltage characteristics allow the observation of voltage gaps whose value is consistent with microscopic results. The data display striking analogies with results obtained on semiconducting multilayers tunnel diodes. Exploring the (5-300)K temperature range, we demonstrate evidence of negative differential conductance with peak currents as high as  $50\mu A$  and voltage discontinuities whose amplitude is in the 50mV-2.5V interval. Based on the effects that these discontinuities generate in the resistance vs. temperature plane we discuss possible switching device applications.

The interest for carbon nanotubes (CNT) in electronic industry has much grown after the fabrication of transistors and diodes based on metal or semiconducting CNT [1]. Recently, fast switching devices consisting of a single bundle showing negative differential conductance (NDC) at room temperature were theoretically predicted [2] and fabricated [3]. NDC devices have a wide impact in electronic industry due to their low switching times as widely demonstrated in semiconducting electronics [4]. In the present paper we report on transport measurements performed on bundles containing semiconducting and metallic single walled (SW) CNT aligned along the bias current direction showing voltage steps as high as  $2.5V$  at  $T=7K$  in the current-voltage ( $I-V$ ) characteristics. The similarity between the obtained curve shapes and that observed in NDC semiconducting devices [6] suggests a tunnel mechanism between SWCNT bundles as a cause of the observed voltage steps.

Bundles of semiconducting and metallic SWCNT [7] were deposited on insulating  $SiO_2$  substrates where metallic Al contacts had been previously patterned with the four lead configuration shown in the inset of Fig.1a. The distance between the main voltage electrodes is  $100\mu m$  while the minimum distance in the corners (see the area inside the white rectangle) is  $5\mu m$ . The bundles were aligned along the arrow direction by a dielectrophoretic technique described elsewhere [8]. The contact geometry allows selecting two different probing configurations referred to as NTPR1 and NTPR2 (NanoTubes Probe 1/2). For the NTPR1 the electrodes P1 and P2 are used as current probes and the electrodes P3 and P6 as voltage probes. For the NTPR2, electrodes P1 and P5 are used for the current injection while P3 and P4 are used as voltage probes. Scanning Electron Microscopy (SEM) revealed that the length of each bundle ranges between  $2\mu m$  and  $3\mu m$  and that their diameter is typically of the order of  $100nm$ ; thus, we found that for the NTPR1 configuration a chain formed by few bundles (in principle even two) would be connecting the voltage electrodes of the corners just as shown in Fig.1a. Instead, for NTPR2 roughly 40 equally spaced parallel chains, each consisting of about 40 aligned bundles, cover the  $100\mu m$  distance between the voltage electrodes P3 and P4. Fig.1b shows two of such parallel bundles, about  $2\mu m$  apart, connected to one of the

electrodes and the inset shows the bundles distribution sampled in an area between the electrodes. Each junction between the bundles generating the chains is supposed to be formed by the action of van der Waals forces between the graphenic surfaces with a consequent potential barrier formation [9].

Transport measurements have been performed in a high vacuum cryocooler equipped for four probe resistance vs. temperature ( $R-T$ ) and  $I-V$  measurements. Fig.2a shows the  $I-V$  characteristics of a NTPR1 configuration measured at  $T=5K$  by current biasing. The curve is rather symmetrical showing that neither metallic contacts nor (insulating) substrate influence the Fermi energy level position with respect to the conduction and valence bands inside the bundles [10]. At low bias current, the  $I-V$  characteristic is ohmic with  $R\cong 90k\Omega$ . Increasing the current up to a peak value  $I_0\cong 0.80\mu A$ , the voltage increases up to  $V_0\cong 70mV$  followed by a voltage jump  $\Delta V\cong 50mV$  with a consequent sharp reduction of the conductance ( $R\cong 150k\Omega$ ). For higher bias current, the ohmic behavior is recovered. The peak current  $I_0$  increases with increasing the temperature as shown in the inset of Fig.2a.

In Fig.2b, the  $I-V$  characteristics of the NTPR2 configuration at different temperatures are reported. As in the case of Fig.2a, an ohmic regime is present at low bias current. A voltage switch occurs at  $V_0\cong 70mV$  for bias current above the peak value  $I_0$ ; increasing the current above this value the transport is governed by thermal assisted tunneling [11]. There are similarities and differences between the results obtained in the NTPR1 and NTPR2 configurations. In particular, the metallic resistance in the low current bias region for NTPR2 is  $R\cong 2k\Omega$  (see Fig.2b) which is much lower than that observed for NTPR1 (see Fig.2a). Moreover, the amplitude of the voltage discontinuity  $\Delta V$  and the current  $I_0$  (compared at the same temperatures) in the NTPR2 configuration are much higher than those of Fig.2a. We also found that  $\Delta V$  and  $I_0$  for NTPR2 are strongly dependent upon the temperature as it is shown in Fig.3a and Fig.3b respectively: here we see that the voltage amplitude  $\Delta V$  of the discontinuity decreases with the temperature according to an exponential law

$\exp(-T/T_0)$  with  $T_0=470K$ . In Fig.3b the continuous line shows the functional dependency of the Anderson's emission model [12] which describes the carrier transport across heterojunctions. Both the dependencies of Fig.3a and Fig.3b indicate that we are dealing with a process in which electrons overcome a barrier energy under the action of an external field [6,12].

Based on the data and analysis presented in the last paragraph, the possible transport mechanism in the samples can be explained following the sketches in the insets of Fig.3 and considering that the voltage step observed for  $V>V_0$  in Fig.2b is much reminiscent of NDC effect reported for current biased semiconducting tunnel diodes [4,6]. At low bias current, the charge transport takes place by tunneling both through metallic and semiconducting SWCNT bundles separated by the junction barriers. In this regime, voltage drop increases linearly with the current and the semiconducting bands start to be misaligned (follow here inset of Fig. 3a from left to right). When  $V=V_0$ , (rightmost picture) the tunneling through semiconducting SWCNT stops because of the complete misalignment of the conduction bands and the current tunnels only through the metallic SWCNT: this phenomenon causes a sharp decrease of the electrical conductance. In this scenario,  $V_0\cong 70mV$  gives the bandwidth and  $\Delta V\cong 50mV$  corresponds to the gap energy in the semiconducting SWCNT. These values are in agreement with spectroscopic measurements performed when curvature effects, surface contacts inside bundles and finite nanotubes length are taken into account [13].

In the case of NTPR2, the higher values of  $\Delta V$  can be interpreted as due to the chains of junctions deposited in parallel between the two voltage electrodes which are spaced  $100\mu m$  away. For these samples (see inset of Fig.3b where each cross represents a junction), the number of junctions is of the order of 40 and a voltage step  $\Delta V=40\times 50mV=2V$  is expected at  $T=5K$ . The measured value of  $2.5V$  at  $T=7K$  in Fig.2b is higher but provides the expected order of magnitude. Moreover, for the 40 parallel bundles chains of the NTPR2 bias configuration, the current value  $I_0=30\mu A$  corresponds to a peak current of  $30\mu A/40=0.75\mu A$  in each bundle chain which is in good agreement with the results shown in Fig.2a.

The large voltage discontinuities observed in our samples offer an interesting applied physics counterpart in terms of switching mechanism. The time required for electrons to transit between the electrodes placed  $5\mu m$  apart in NTPR1 can be roughly estimated by summing the time to move along two nanotubes of  $2\mu m$  at the Fermi velocity  $v_F=8.1\cdot 10^5 m/s$  and the tunneling time given by the uncertainty relation  $\tau=\hbar/e\Delta V$  where  $\hbar$  is the Planck constant divided by  $2\pi$ ,  $e$  the electron charge and  $\Delta V\cong 50mV$ . The calculation gives  $\tau\cong 2\cdot 10^{-12}s$  as switching time which is of the same order of the fastest semiconducting based switching devices.

The data shown in Fig.2 suggest an interesting application of the samples as temperature sensitive switching devices. In Fig.4 the  $R$  vs.  $T$  curves are reported for the NTPR2 configuration for three different values of the d.c. bias current  $I_{bias}$ . When the  $I_{bias} = 50\mu A$ , well above the  $I_0$  range shown in Fig.3b, a typical semiconducting behavior is observed [11]. When  $I_{bias}=20\mu A$  is below of  $I_0$  an ohmic behavior is recorded. Instead, when  $I_{bias}=30\mu A$  is close to  $I_0$ , a large step in the resistance is observed. The step in the resistance and the temperature value where this step is observed depend on the bias current used and we found that the dependence of the switchings on the specific current value was highly reproducible. We note that the contact barriers were generated just by the overlapping of the bundles during alignment and no further processing was required; thus, the switching currents of the devices could just be tuned by increasing the density of bundles in the fabrication procedure and the switching voltages could be tuned by adequately selecting the length between the electrodes. This relative ease in the fabrication process and in the “a priori” determination of the characteristics of the samples are particularly stimulating in view of device applications.

In conclusion, we have reported on the negative differential conductivity effects in bundles of SWCNT. The measured voltages discontinuities are consistent with the microscopic evaluation of energy gaps for nanotube bundles. The amplitude of the voltage discontinuity, occurring when the feeding currents become larger than a threshold value, is found to be an increasing function of the

number of the bundles connected in series between the voltage probes. The overall reliability of the samples is very encouraging in view of applications as voltage switches and low temperature sensors.

We are grateful to Prof. C. Attanasio at University of Salerno (Italy) for helpful discussions and comments.

## References

- [1] S.J. Tans, A.R.M. Verschueren and C. Dekker, *Nature* **393**, 49(1998); M. Rinkio, A. Johansson, G.S. Paraoanu, P. Törma, *Nano Letters* **9**, 643(2009).
- [2] S. Maksimenko, G. Y. Slepyan, *Phys. Rev. Lett.* **84**, 362(2000).
- [3] G. Buchs, P. Ruffieux, P. Groning, O. Groning, *Appl. Phys. Lett.* **93**, 73115(2008); M. Dragoman, G. Konstantinidis, A. Kostopoulos, D. Neculoiu, R. Buiculescu, R. Plana, F. Coccetti, H. Hartnagel, *Appl. Phys. Lett.* **93**, 43117(2008).
- [4] D.K. Ferry and S.M. Goodnik, *Transport in nanostructures*, Cambridge University Press (2001).
- [5] R. Saito, G. Dresselhaus, and M. Dresselhaus, *Physical Properties of carbon nanotubes*, Imperial College, London (1998).
- [6] R.A. Davies, M.J. Kelly, T.M. Kerr, *Phys. Rev. Lett.* **55**, 1114(1985).
- [7] B. Mateusz, B. Bryning, M.F. Islam, J.M. Kikkawa, A.G. Yodh, *Adv. Mater.* **17**, 1186(2005).
- [8] M.L. Terranova, M. Lucci, S. Orlanducci, E. Tamburri, V. Sessa, A. Reale, A. Di Carlo, *J.Phys.D: Condensed Matter* **19**, 2255004 (2007).
- [9] J.C. Charlier, X. Blasé, S. Roche, *Rev. Mod. Phys.* **79**, 677(2007).
- [10] J.W.G. Wildoer, L.C. Venema, A.G. Rinzler, R.E. Smalley, C. Dekker, *Nature* **391**, 59(1998).
- [11] M. Salvato, M. Cirillo, M. Lucci, S. Orlanducci, I. Ottaviani, M.L. Terranova, F. Toschi, *Phys. Rev. Lett.* **101**, 246804(2008).
- [12] L.W. Liu, J.H. Fang, L. Lu, F. Zhou, H.F. Yang, A.Z. Jin, C.Z. Gu, *Phys. Rev.* **B71**, 155424(2005); G. Margaritondo, *Electronic Structure of Semiconductor Heterojunctions* Ed. Kluwer, Boston (1988).
- [13] M.S. Fuhrer, J. Nygard, L. Shih, M. Forero, Y-G. Yoon, M.S.C. Mazzoni, H.J. Choi, J. Ihm, S.G. Louie, A. Zettl, P.L. McEuen, *Science* **288**, 494(2000).

## Figure Captions

Figure 1. a) SEM image showing two bundles chain for NTPR1 with the arrow indicating the position of the junction; inset: schematic of the four leads configuration. The arrow indicates the CNT alignment direction; b) SEM image showing two parallel chains departing from the aluminium contact pad for NTPR2. The inset shows the bundles in a region between the electrodes.

Figure 2. a)  $I$ - $V$  characteristic for NTPR1 measured at  $T=5K$ . Inset: temperature dependence of the peak current  $I_0$ ; b)  $I$ - $V$  characteristics at different temperatures for a NTPR2 probing configuration.

Figure 3. Temperature dependence of (a) the voltage step  $\Delta V$  and (b) the peak current  $I_0$  for the NTPR2 configuration. Insets: a) sketch of the suggested transport mechanism and b) series-parallel junction configuration for NTPR2

Figure 4.  $R$ - $T$  dependence in the NTPR2 for three different values of the bias current.



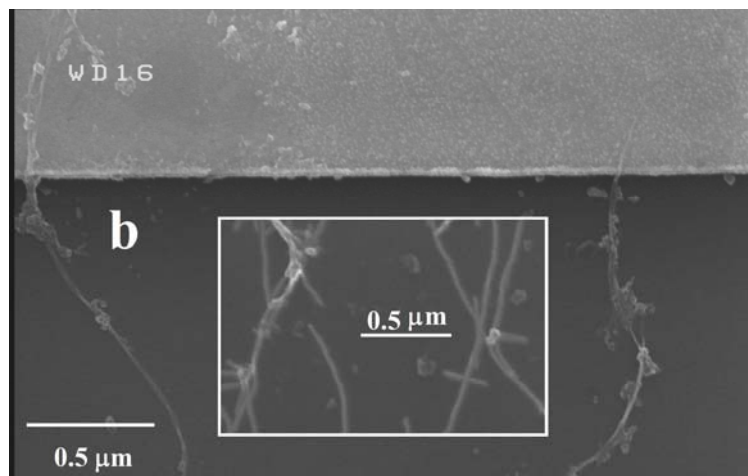
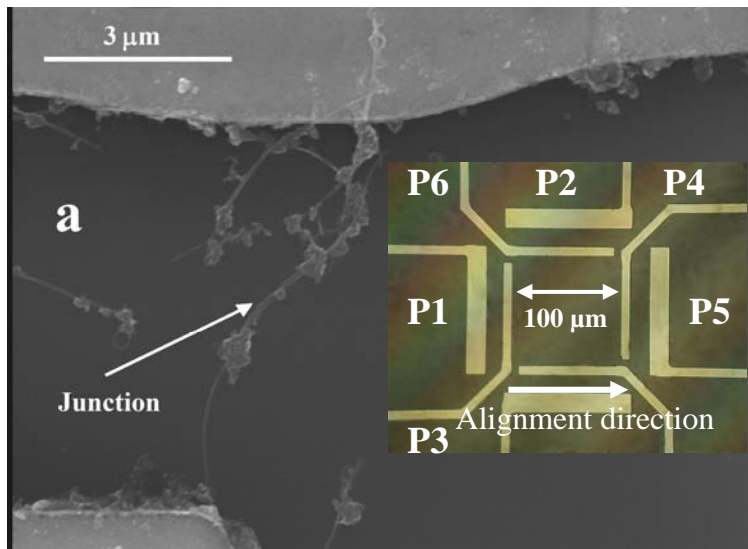


Figure 1, M. Salvato et al.

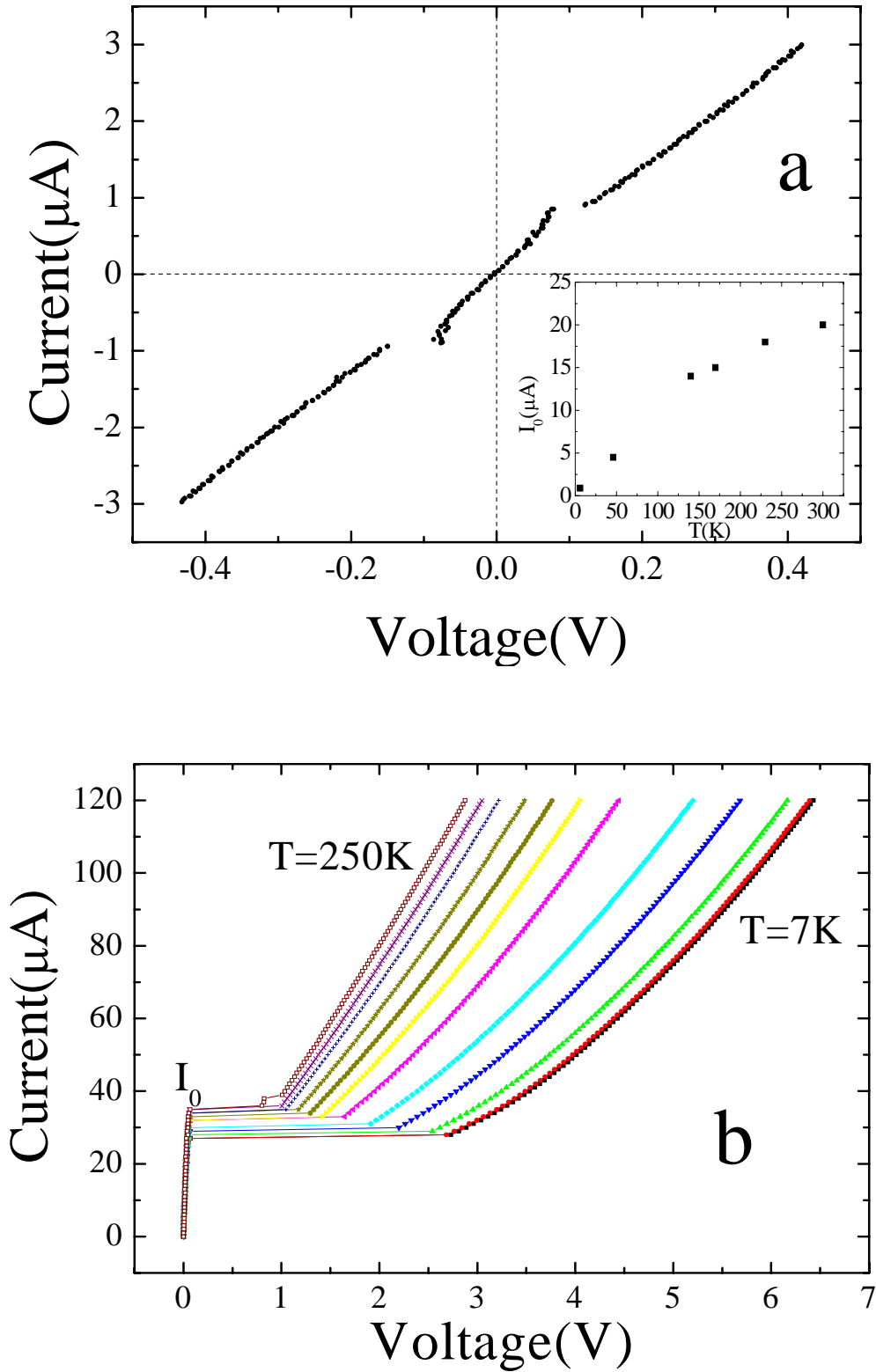


Figure 2, M. Salvato et al.

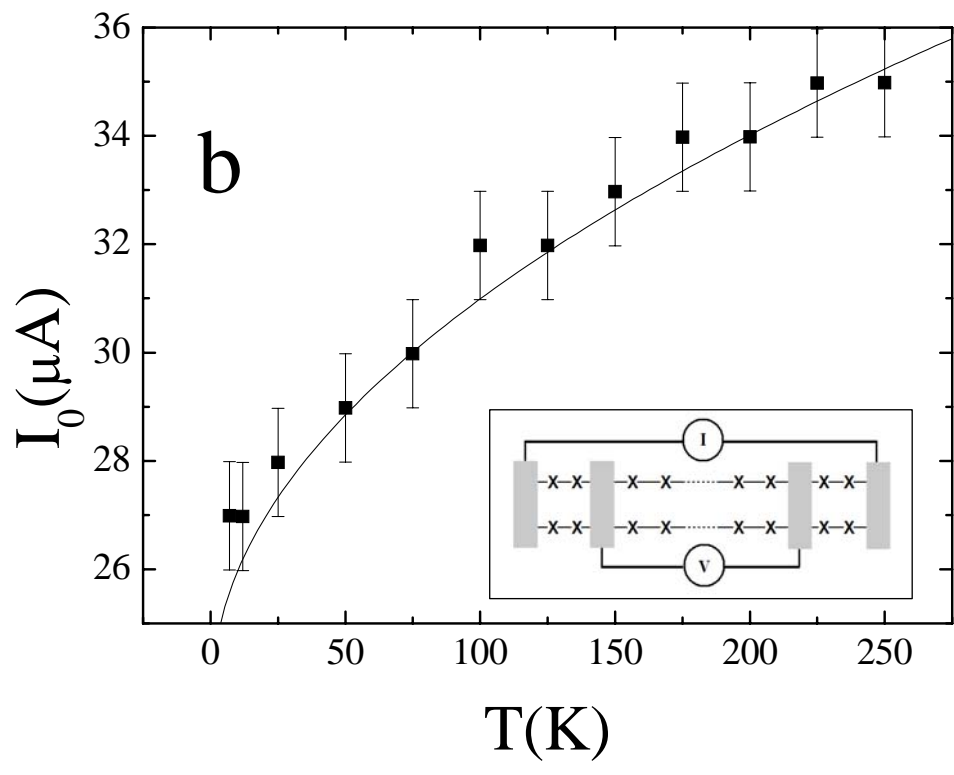
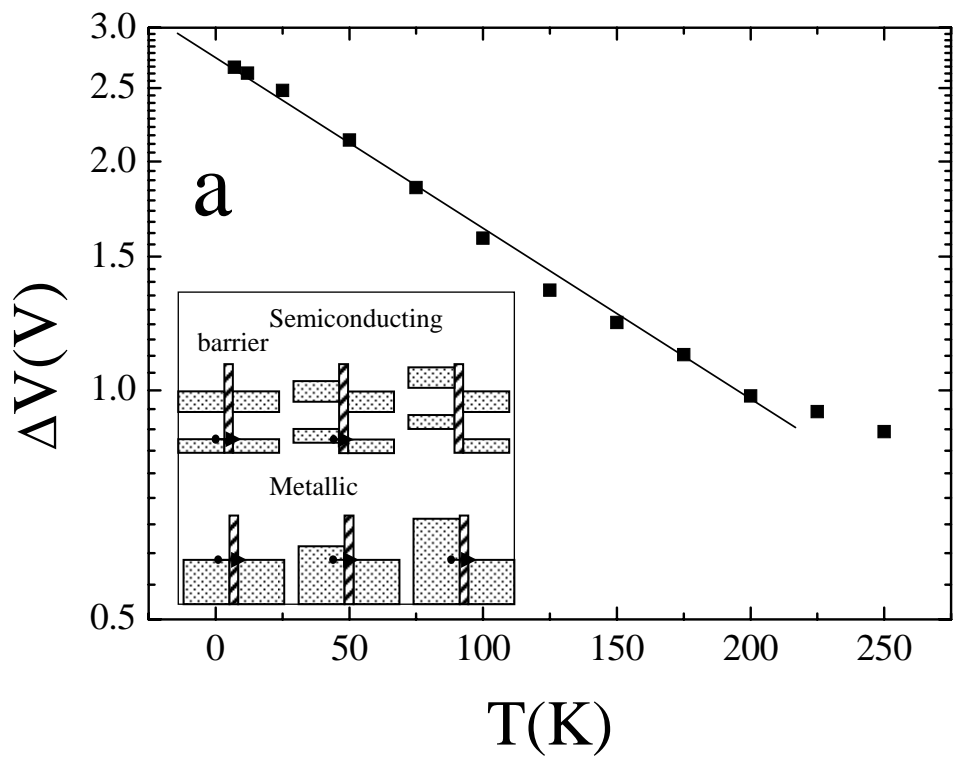


Figure 3, M. Salvato et al.

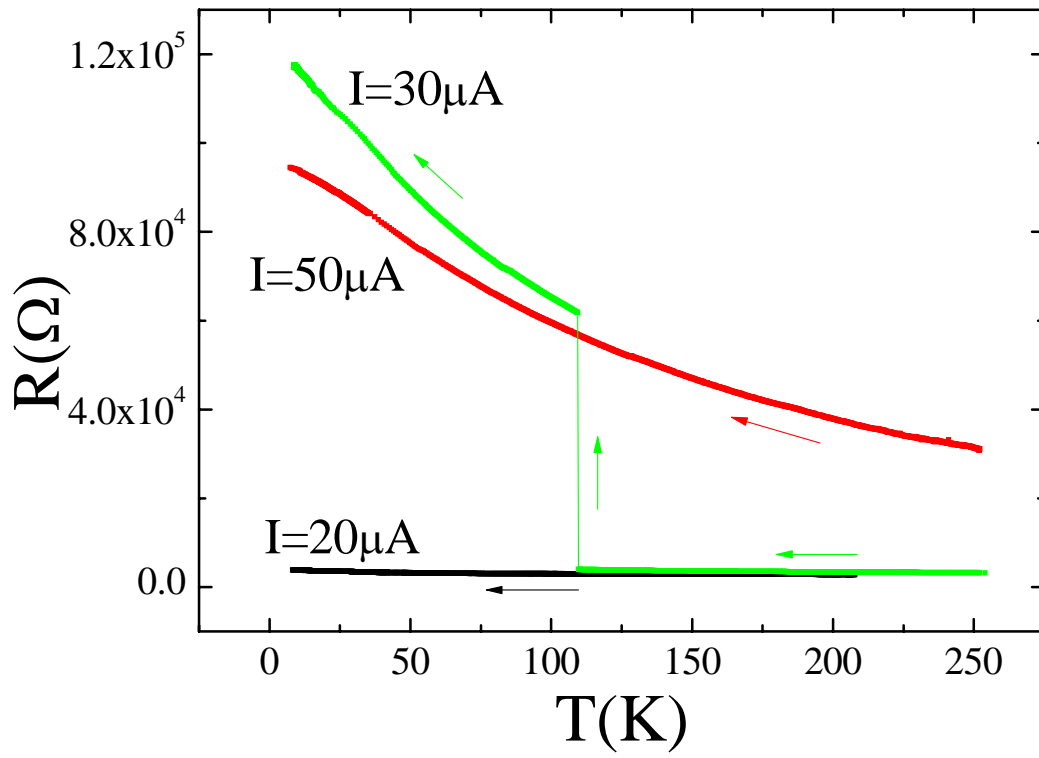


Figure 4, M. Salvato et al.